JOURNAL OF SOLID STATE CHEMISTRY 71, 19–28 (1987)

Layered Alkali Rhodium Oxides A_xRhO_2: Topotactic Solvation, Exchange, and Redox Reactions

A. MENDIBOURE, H. EICKENBUSCH, AND R. SCHÖLLHORN*

Institut für Anorganische und Analytische Chemie, Technische Universität Berlin, Straße des 17. Juni 135, D-1000 Berlin 12, West Germany

AND G. V. SUBBA RAO

Materials Science Research Centre, Indian Institute of Technology, Madras 600 036 India

Received June 13, 1986; in revised form December 8, 1986

The intercalation/deintercalation properties of the layered oxides $LiRhO_2$, $NaRhO_2$, and $KRhO_2$ have been investigated with respect to redox and exchange processes. The chemical reactivity was found to be strongly dependent upon the alkali cation. Only $KRhO_2$ is able to form hydrated phases and to undergo quantitative K^+/H^+ exchange, resulting in the formation of the new layered hydrogen bronze $HRhO_2$. $HRhO_2$ has a limited phase range up to $H_{1.1}RhO_2$ and exhibits no Brönsted acid character. $LiRhO_2$ and $NaRhO_2$ both show a limited cycling range in aprotic Li^+ or Na^+ electrolytes beyond which irreversible lattice disorder is observed. The origin of the significant differences in topotactic reactivity between layered dichalcogenide and oxide systems is discussed.

Introduction

The chemical reactivity of layered ternary chalcogenides A_xMX_2 (A = alkali metal, M = transition element, X = S, Se) with respect to topotactic processes at room temperature has been investigated in some detail (*1–5*). Characteristic features of these systems are (i) the high and selective translational mobility of the alkali atoms A^+ between the CdI_2- or MoS_2-type $[MX_2]^{x-}$ layer matrix units (two-dimensional diffusion), (ii) reversible redox reactions of the type

$$A^+[MX_2]^{x-} \rightleftharpoons A^+_{x-z}[MX_2]^{(x-z)-} + zA^+ + ze^-, \quad (1)$$

(iii) the reaction of these phases with polar solvents (e.g., H_2O) to solvated phases

$$A^+_x[MX_2]^{x-} + y\ \text{solv} \rightleftharpoons A^+_x(\text{solv})_y[MX_2]^{x-}, \quad (2)$$

and (iv) polyelectrolyte behavior, i.e., cation and solvent exchange properties. In order to expand our knowledge on these systems and to compare series with layer anions X of different electronegativity it is of particular interest to examine the reactivity of the related oxo compounds A_xMO_2 which exhibit structures closely related to those of the chalcogenides. Several studies have actually been reported on layered oxides but these were restricted essentially to the redox properties (Eq. (1)) of lithium and so-

* To whom correspondence should be addressed.

0022-4596/87 $3.00

dium compounds Li_xMO_2/Na_xMO_2 with first row transition elements (*6–8*). We have become interested in phases with 4*d* and 5*d* metals and the question whether polyelectrolyte behavior can be observed also for the oxide series. Moreover, our attention was focused on the possibility of preparing hydrogen bronzes H_xMO_2 via desolvation or potential hydronium compounds and on electron/proton transfer processes. We report here on the results of an investigation of the ternary alkali rhodium oxometallates $ARhO_2$ (A = Li, Na, K) which demonstrate that the topotactic reactivity of these layered oxides is strongly dependent upon the nature of the alkali ion.

Experimental

The ternary phases $ARhO_2$ were prepared by heating a mixture of the corresponding alkali carbonate A_2CO_3 (A = Li, Na, K) with Rh_2O_3 at a ratio 1 : 1 to a temperature of 900°C in a dry oxygen atmosphere. The rhodium oxide was obtained by oxidation of pure rhodium powder (99.95%) in an oxygen atmosphere at 950°C. After 24 hr, the material obtained was ground in an agate ball mill and reheated for 24 hr. Alkali carbonates were dried for 15 hr at 150°C in air before use. The ternary phases were recovered under an inert gas atmosphere and manipulated in a glove box. Analytical data were obtained by atomic absorption spectrometry (Rh, Li, Na, K) and combustion microanalysis (hydrogen; error 0.03% wt). The following values (wt%) resulted for the oxometallates $ARhO_2$:

	A		Rh	
	Found	Calc	Found	Calc
$LiRhO_2$	4.88	4.89	72.57	72.55
$NaRhO_2$	14.60	14.56	65.20	65.18
$KRhO_2$	22.45	22.47	59.16	59.14

Structural characterization was achieved by X-ray Guinier powder diagrams; samples susceptible to air were sealed in lithium borate glass capillaries.

Electrochemical reactions were carried out at 300 K in three electrode cells either in aprotic organic electrolytes (propylene carbonate, $LiClO_4$ or $NaClO_4$) with the alkali metals as counter and reference electrodes or in aqueous electrolytes with a Ag/AgCl reference electrode. Working electrodes consisted of pressed polycrystalline materials on platinum grids. A computer-controlled system was used for cycling experiments in galvanostatic or potentiostatic mode.

Results and Discussion

The three alkali oxorhodates $LiRhO_2$, $NaRhO_2$, and $KRhO_2$ are isostructural with α-$NaFeO_2$ (Fig. 1) (*9*). Their highly anisometric structure can be described by a stacking of $[RhO_2]$ sheets with three sheets per unit cell. The CdI_2-type layer units are built up of (RhO_6) octahedra sharing edges. They are characterized by a negative excess charge $[RhO_2]^{1-}$ which is compensated by the alkali atoms that are located on octahedral sites between the macroanion

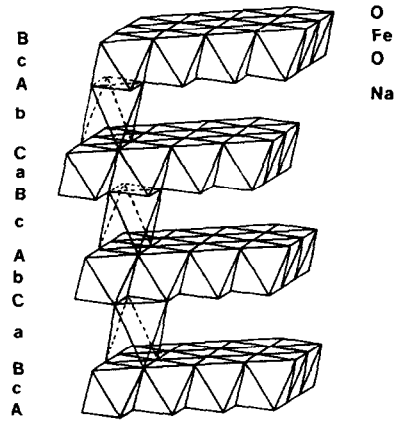

Fig. 1. Structure scheme of α-$NaFeO_2$ (*9*).

TABLE I

HEXAGONAL (h) AND ORTHORHOMBIC (o) LATTICE PARAMETERS OF LAYERED TERNARY RHODIUM OXIDES $ARhO_2$

		a_h (Å)	c_h (Å)	a_o (Å)	b_o (Å)	c_o (Å)	d (Å)
$LiRhO_2$	[1]	3.018	14.195	5.227	9.060	28.39	4.73
$NaRhO_2$	[1]	3.090	15.491	5.350	9.267	30.98	5.16
$KRhO_2$	[1]	3.066	15.696	5.319	9.188	31.33	5.23
"$KRhO_2$"	[2]	3.068	20.63	5.327	9.202	41.00	6.82

Note. A = Li, Na, K; d = intersheet distance = $c_h/3$; [1] data of present work, [2] data calculated from diffraction lines reported in Ref. (*10*).

sheets. The refined lattice parameters of the alkali phases are given in Table I in hexagonal (space group $R\bar{3}m$) and orthorhombic setting; the two cells are converted by the following relations: $a_h = a_0/\sqrt{3}$, $a_h = b_0/3$, $c_h = c_0/2$. The values obtained are in good agreement with those in the literature (*11*, *12*) with the exception of $KRhO_2$ which exhibits a c axis considerably lower than that reported earlier (*10*, cf. Table I). As compared to $LiRhO_2$ and $NaRhO_2$, the interlayer spacing d (distance between neighboring RhO_2 sheets perpendicular to the basal plane) observed by us for $KRhO_2$ seems to be compatible with the ionic radius of K^+, after Shannon and Prewitt (*13*). An explanation for the higher value reported in Ref. (*10*) is given below. According to (*10*) the three ternary phases exhibit semiconductor properties.

Previous work on AMO_2 phases with $3d$ row elements has shown that reversible structural transitions involving gliding of the MO_2 planes along directions perpendicular to the stacking axis appear in the course of deintercalation and intercalation (*6*, *7*). Such stacking changes have a low activation energy and can take place at room temperature. The covalency of the Rh–O bonding is higher as compared to M–O bonding with $3d$ elements, which reduces the effective negative charge on the oxygen atoms for the Rh–O system; it can be expected that this may affect the activation energy for stacking changes. Similarly one could expect a higher maximum oxidation state for Rh on oxidative deintercalation (Eq. (3)) since the stability of higher oxidation states

$$A_1^+[RhO_2]^- \underset{\text{red.}}{\overset{\text{ox.}}{\rightleftharpoons}} A_x^+[RhO_2]^{x-} + (1-x)e^- + (1-x)A^+ \quad (3)$$

increases within the transition element groups with increasing atomic number.

$LiRhO_2$ and $NaRhO_2$

The redox reactions of $LiRhO_2$ have been studied electrochemically in a galvanic cell of the type $Li^0//LiClO_4$, propylenecarbonate//$LiRhO_2$ in aprotic electrolytes. A typical oxidation and reduction curve (galvanostatic cycling) is shown in Fig. 2. The maximum accessible positive potential is limited by the kinetic potential of electrolyte decomposition (*14*). Analytical studies confirmed that the correlation between the electrochemical charge transfer n (e^-/$LiRhO_2$) and the analytical Li content in Li_xRhO_2 was linear (1 : 1) up to a potential of 4 V vs Li^0; i.e., the reaction proceeds formally according to Eq. (3). In Fig. 2 a large voltage difference is observed between the

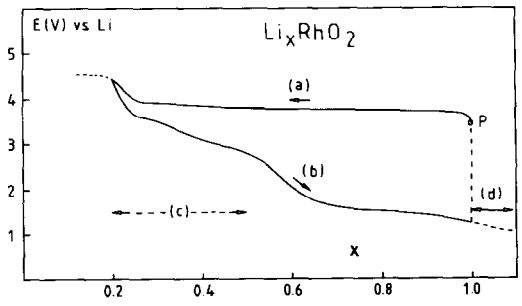

Fig. 2. Cycling diagram of $LiRhO_2$ electrodes in Li ClO_4/PC electrolyte (galvanostatic mode); P = starting potential; E = potential versus reference electrode; x = stoichiometric index of Li_xRhO_2. (a) Oxidation, (b) reduction, (c) range in which amorphous phase appears, (d) limited range with $x > 1$. $I = 30\ \mu A/cm^2$.

oxidation and reduction curves, which results from the low electronic conductivity of Li_xRhO_2. The potential plateau which appears at 3.7 V vs Li in the oxidation curve is not observable in the reduction curve. A two-phase region is therefore unlikely to exist. Structural studies showed, in fact, that with decreasing x values a strong broadening of the X-ray lines appears. At the composition $Li_{0.2}RhO_2$ the material becomes strongly disordered and the only observable diffraction line left corresponds to the interlayer distance of the starting material (d = 4.73 Å). On cathodic reduction of the oxidized product no clear endpoint appears and the consumption of more than 1 e^- can be observed.

The increasing disorder of the system upon oxidation cannot be explained in a simple way in terms of statistical stacking defects only (one-dimensional disorder). We assume that with increasing concentration of Rh^{4+} within the layers, the increasing repulsion of the highly charged transition metal atoms leads to a relaxation of the lattice via irreversible translation of a fraction of the rhodium atoms to vacant octahedral sites in the interlayer space. This process should be facilitated in the $LiRhO_2$ case by the low interlayer distance (due to the small size of Li^+) which provides octahedral sites between the layers with low symmetry distortion and Rh–O distances comparable to those of Rh within the layers. Simultaneously the small size and high mobility of Li favors the necessarily correlated diffusion of Li to octahedral sites within the layer units.

In contrast to $KRhO_2$ (cf. below) the lithium phase $LiRhO_2$ does not show spontaneous hydration in air or ion exchange in neutral aqueous electrolytes. Although this could be attributed to kinetic aspects (strong change in interlayer distance upon the uptake of H_2O or larger cations) we assume that structural aspects are also involved. Due to the comparable size of Li^+ and Rh^{3+} lattice sites and ionic diameters, it is possible that the stoichiometric phase $Li[RhO_2]$ already shows lattice disorder of the type $Li^+_{1-x}Rh^{3+}_x[Rh^{3+}_{1-x}Li^+_xO_2]$. Even for very small x values the presence of trivalent metal atoms in the interlayer space must lead to a tremendous increase in activation energy for an increase in layer spacing required upon intercalation of larger guest molecules or ions. A similar case has recently been observed in the series $LiCrS_2$, $NaCrS_2$, and $KCrS_2$, where the K^+ phase shows a high reactivity for solvation and exchange reactions while the Li phase is inert (*15, 16*). It should be possible, however, to replace Li^+ ions in $LiRhO_2$ by ions of smaller size via exchange reaction. This has in fact been observed: treatment of the lithium compound with aqueous mineral acids at 50–100°C for extended times results in partial exchange under formation of $Li_{0.6}H_xRhO_2$ ($x \simeq 0.4$), whose lattice parameters are identical to those of $LiRhO_2$ within the limits of error.

The anodic oxidation and reduction of $NaRhO_2$ electrodes in a galvanic cell

$$Na^0//NaClO_4,\ \text{propylene carbonate}//NaRhO_2,$$

is shown in Fig. 3. The reversible range observed for Na_xRhO_2 is $0.4 \leqq x \leqq 1$. At

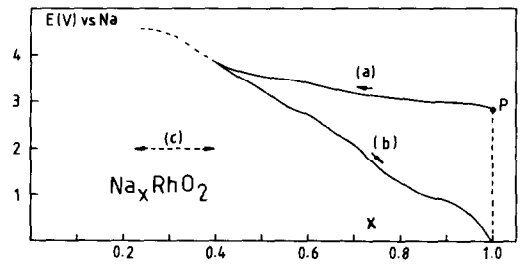

Fig. 3. Cycling diagram of $NaRhO_2$ electrodes in $NaClO_4$/PC electrolyte (galvanostatic mode); E = potential versus reference electrode; x = stoichiometric index (Na_xRhO_2); P = starting potential. (a) Oxidation, (b) reduction, (c) range in which amorphous phase appears. I = 30 μA/cm^2.

lower x values or at current densities $\gg 30$ $\mu A/cm^2$ line-broadening due to lattice disorder is found. The potential curve (E/x) suggests a continuous nonstoichiometric region for the accessible topotactic range; this is supported by the structural data (Fig. 4), which show that the reaction proceeds under retention of the lattice integrity with a continuous change in lattice parameters with the oxidation state. The hexagonal c axis increases with decreasing Na content. As in the related reaction of other lamellar structures (*6–8*), this is a consequence of uncompensated repulsion of the oxygen layers and decreasing electrostatic attraction. The change in the a axis corresponds to a variation of the O–O distances within the $[RhO_2]$ sheets. On deintercalation, the relative amount of Rh(IV) ions increases and leads to a higher covalency of the Rh–O bonds, resulting in a contraction of the RhO_6 octahedra and thus a reduced a axis value. The ABCABC stacking mode of the layers (structural type *O*3) remains unaltered in the course of intercalation and deintercalation. This is a characteristic difference to Na_xMO_2 oxides of 3*d* elements (M = Cr, Co, Ni) which undergo reversible structural transitions to an ABBCCA stacking sequence (*P*3) (*6*).

The strong difference in potential between oxidation and reduction half cycles is due to the low electronic conductivity of the material. The efficient reversibility of the system Na_xRhO_2 over a relatively wide range of composition must be correlated to the absence of stacking transitions in the course of the reaction cycle.

Similar to the lithium phase the sodium compound $NaRhO_2$ is stable in air and water at ambient temperature. However, upon treatment at elevated temperature with aqueous mineral acids (1 M H_2SO_4, 100°C, 48 hr) a phase with a ratio Na/Rh $\simeq$ 0.70 is obtained with lattice parameters identical to those of the starting phase. Hydrogen analysis showed that a mixed sodium/hydrogen compound, $Na_{0.7}H_{0.3}RhO_2$, is formed.

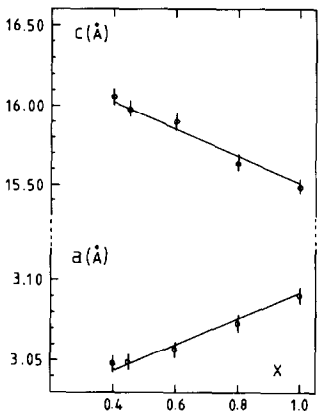

Fig. 4. Change of hexagonal lattice parameters a and c with the stoichiometry x in Na_xRhO_2.

$KRhO_2$

Unlike the lithium and sodium phases, the black $KRhO_2$ was found to react spontaneously with water on exposure to air with increasing interlayer spacing. Treatment with water and subsequent drying in air results in the formation of a dark brown hydrated compound with the composition $K_{0.4}H_x(H_2O)_{0.5}[RhO_2]$. Although the value of x again could not be determined accurately it is very likely that x is equal to 0.6; i.e., rhodium has an integral valency of 3 (Eq. (4)):

$$KRhO_2 + 1.1H_2O \rightarrow K_{0.4}H_{0.6}(H_2O)_{0.5}[RhO_2] + 0.6KOH. \quad (4)$$

This is concluded from the fact that the potentials of the pristine $KRhO_2$, of the hydrated phase, and of $HRhO_2$ (cf. below) in aqueous electrolytes versus Ag/AgCl are very similar. The water content may vary slightly depending upon the ambient vapor pressure. The c axis of the hydrated phase is very close to the c axis for "$KRhO_2$" reported by Lazarev and Shaplygin (*10*) (Table I). We conclude therefore that the

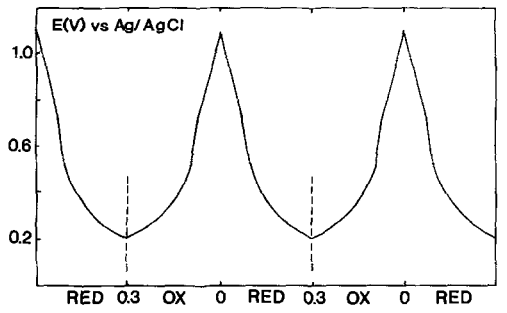

Fig. 5. Cycling diagram for $K_{0.4}(H_2O)_{0.5}H_{0.6+x}RhO_2$ in 0.1 *N* aqueous H_2SO_4. Current density = 30 $\mu A/cm^2$; cycling range = 0.3 e^-; i.e., $0 \leqq x \leqq 0.3$.

material measured by these authors was the hydrated phase. The X-ray diffraction pattern of $K_{0.4}H_{0.6}(H_2O)_{0.5}[RhO_2]$ could be indexed with a hexagonal unit cell. The increase in interlayer distance from $d = 5.23$ Å ($KRhO_2$) to $d = 6.74$ Å (hydrated phase) is essentially due to the uptake of a (partial) monomolecular layer of water molecules between the (RhO_2) sheets. This hydrated phase could be electrochemically reduced in aqueous electrolytes (0.1 *N* H_2SO_4) as shown in Fig. 5. A very good reversibility is obtained for a reduction/oxidation range of 0.3 e^-/mole. The fully reduced phase retains a hexagonal cell with a slight increase of the interlayer distance to $d = 6.89$ Å (Table II).

There are two possible sites for the hydrogen atoms either in direct (covalent) bonding to the layer oxygen atoms or bonded to the H_2O solvate molecules as H_3O^+, represented by the general formulae

$$K_x^+(H_2O)_y[H_zRhO_2]^{x-}$$

or

$$K_x^+(H_3O^+)_y[RhO_2]^{(x+y)-}$$

and leading to different formal negative excess charges of the layer matrix. The first formula is more likely in view of the low acidity of O–H groups.

The easy hydration reaction of $KRhO_2$ as opposed to the Li and Na phases is explained in terms of two aspects: (i) the high interlayer spacing strongly reduces the activation energy for the insertion of molecular species such as water with an effective diameter similar to K^+; and (ii) the high interlayer spacing renders the existence of K/Rh disorder unlikely due to the unfavorable coordination of Rh in the interlayer region at higher *d* values.

The composition of the hydrated phase is close to a ratio $K/H_2O = \frac{1}{2}$. This leads to an energetically favored situation since the K/H_2O sublattice structure can remain hexagonal with an optimal coordination for every K^+ by six H_2O molecules within the interlayer space and three layer oxygens above and below (i.e., KO_{12} polyhedra) and a minimum K^+/K^+ repulsion.

No solvate exchange has been observed for the hydrated phase with organic polar solvents (e.g., dimethyl sulfoxide, *n*-methylformamide), and ion exchange reactions were found to proceed very slowly. The exchange, e.g., of K^+ for Cs^+ leads after several weeks to the hydrated cesium phase with the hexagonal lattice parameters $a = 3.054$ Å, $c = 21.52$ Å, and an interlayer spacing $d = 7.12$ Å, which is a slight increase in *d* relative to the hydrated K phase as expected.

$HRhO_2$

Both the ternary phase $KRhO_2$ and the hydrated phase were found to react with dilute aqueous mineral acids in air at 100°C

TABLE II

HEXAGONAL (h) LATTICE PARAMETERS OF $KRhO_2$ AND HYDRATED DERIVATIVES

		a_h (Å)	c_h (Å)	d (Å)
Starting material	$KRhO_2$	3.066	15.696	5.23
Hydration	$K_{0.4}H_{0.6}(H_2O)_{0.5}RhO_2$	3.060	20.21	6.73
Reduction	$K_{0.4}H_{0.9}(H_2O)_{0.5}RhO_2$	3.066	20.68	6.89

Note. $d = c/3$ = interlayer distance.

within 80 hr by quantitative exchange of K^+ for protons via an unstable hydrated phase (lattice parameters identical to those of the hydrated K phase) to a brown hexagonal hydrogen compound with the analytical composition H_1RhO_2, according to Eqs. (5) and (6). This hydrogen bronze is metastable,

$$KRhO_2 + H_3O^+ \rightarrow (H_2O)[HRhO_2] + K^+ \quad (5)$$

$$H_2O[HRhO_2] \rightarrow HRhO_2 + H_2O. \quad (6)$$

DTA/DTG data indicate an endothermic irreversible transformation at 410°C leading to the formation of Rh_2O_3 and H_2O:

$$2HRhO_2 \rightarrow Rh_2O_3 + H_2O. \quad (7)$$

In order to obtain a comparison with the related A_xCoO_2 system, we investigated the reaction of the ternary sodium oxocobaltates with aqueous mineral acids. Although the basic reactivity, i.e., formation of hydrogen phases, is very similar to that of $KRhO_2$ there are differences depending upon the stoichiometry of the ternary cobalt phases. The results are presented in Table III. It is interesting that although one would expect in the case of $Na_{0.75}CoO_2$ and $Na_{0.55}CoO_2$ the formation of $H_{0.75}CoO_2$ and $H_{0.55}CoO_2$, only the compositions $H_{0.95}CoO_2$ and $H_{0.90}CoO_2$ are found. This means that Co(IV) oxidizes H_2O to O_2 and is reduced to Co(III).

The X-ray diffraction data of the H_xCoO_2 phases obtained are identical to the data published by Deliens and Goethals (*22*) and Kondrashev and Fedorova (*23*) who synthetized $HCoO_2$ compounds hydrothermally by aging $Co(OH)_2$ in water at 100°C. The two hydrogen phases $H_{0.95}CoO_2$ (*P*3) and $H_{0.90}CoO_2$ (*P*2) have linear O–H · · · O hydrogen bonds. However, while $Na_{0.95}CoO_2$ and $Na_{0.75}CoO_2$ both undergo a stacking change $O3 \rightarrow P3^*$ it is found that $Na_{0.55}$

TABLE III

EXCHANGE REACTIONS OF LAYERED A_xMO_2 PHASES

	Starting composition			
	$Na_{0.95}CoO_2$	$Na_{0.75}CoO_2$	$Na_{0.55}CoO_2$	$KRhO_2$
Oxygen stacking	ABCABCAB	ABCABCAB	ABBAAB	ABCABCAB
Structural type	*O*3	*O'*3 monoclinic distortion	*P*2	*O*3
Unit cell parameters	$a_h = 2.886$ $c_h = 15.58$	$a_m = 4.890$ $b_m = 2.866$ $c_m = 5.77$ $\beta_m = 111.28°$	$a_h = 2.829$ $c_h = 10.89$	$a_h = 3.066$ $c_h = 15.69$
Intersheet distance	$d = 5.19$	$d = 5.37$	$d = 5.44$	$d = 5.22$
	Exchange product			
	$H_{0.95}CoO_2$	$H_{0.95}CoO_2$	$H_{0.90}CoO_2$	$HRhO_2$
Oxygen stacking	ABBCCAAB	ABBCCAAB	ABBAAB	ABBCCAAB
Structural type	*P*3*	*P*3*	*P*2*	*P*3*
Unit cell parameters	$a_h = 2.853$ $c_h = 13.13$	$a_h = 2.855$ $c_h = 13.15$	$a_h = 2.847$ $c_h = 8.87$	$a_h = 3.096$ $c_h = 13.406$
Interlayer distance	$d = 4.37$	$d = 4.38$	$d = 4.43$	$d = 4.46$

Note. *M* = Co, Rh, *A* = Na, K; lattice parameters given in Å; * = protons in linear coordinations O–H · · · O; h = hexagonal; m = monoclinic.

CoO_2 with $P2$ structure exhibits a transition $P2 \rightarrow P2^*$. This is in agreement with previous work which demonstrated that a stacking transition $P2 \rightarrow P3^*$ is not possible (*8*) and explains that in the case of $Na_{0.55}CoO_2$ the resulting hydrogen phase retains the original $P2$ structure of the starting compound. (In the structural notation used (*O3*, *P3*, *P2*), the letter *O* or *P* accounts for the alkali ion site (octahedral or prismatic) and the following number indicates how many sheets are contained in the crystallographic unit cell.)

Since $KRhO_2$ is isostructural with $Na_{0.95}CoO_2$ (*O3*) and $Na_{0.75}CoO_2$ (*O'3*), it is reasonable to infer that exchange reactions of alkali ions for protons lead to similar structural modifications. We assume therefore that $HRhO_2$ exhibits the same linear O–H · · · O hydrogen bonds as H_xCoO_2. The resulting structural transition should be $O3 \rightarrow P3^*$. The intersheet distance which we observe for $HRhO_2$ (Table III) is in fact very close to the values observed in H_xCoO_2. The minor increase results from the larger size of rhodium as compared to cobalt.

X-ray powder diffraction data of $HRhO_2$ are given in Table IV. The compound is hexagonal and exhibits a decrease in interlayer spacing of $\Delta d = 0.76$ Å as compared to $KRhO_2$ (Table III). Model calculations with the X-ray intensity data of $HRhO_2$ have been based on the space group $R\bar{3}m$ and the atomic positions reported in the literature for $HCrO_2$ ($P3$-type) (*17*, *18*). Although calculations performed with the first four reflections are in good agreement with a $HCrO_2$-type structure, the use of all intensity data resulted in poor R values. We consider this a consequence of texture effects (preferential orientation of the anisometric crystallites) and to line-broadening due to lattice disorder.

The spontaneous dehydration of the hydrated rhodium phase at 100°C (Eq. (6)) is not reversible at room temperature in aqueous electrolytes. Also $HRhO_2$ does not react as a solid Brönsted acid with alkali hydroxides or Lewis bases as observed for chalcogenide hydrogen bronzes H_xMX_2 (*4*). This can be understood in terms of strong linear O–H · · · O bonds between the (RhO_2) layers in the hydrogen phase and the low acidity of the Rh(III)–O–H groups. Electrochemical reduction of $H_{1.0}RhO_2$ in acid electrolytes is reversible (Eq. (8)) but the range observed $0 \leqq x \leqq 0.1$ is significantly smaller compared to the reduction of the hydrated phase $K_{0.4}H_{0.6}(H_2O)_{0.5}(RhO_2)$:

$$H_1RhO_2 + xe^- + xH^+ \rightleftharpoons H_{1+x}RhO_2. \quad (8)$$

Here again the interpretation can be based upon structural aspects: in $HRhO_2$ all layer oxygens are assumed to be engaged in O–H · · · O bonding and the insertion of additional H atoms is obviously energetically and structurally unfavorable. In $K_{0.4}H_{0.6}(H_2O)_{0.5}[RhO_2]$ no linear O–H · · · O bonds are possible and "free" layer oxygen sites

TABLE IV

X-RAY POWDER DIFFRACTION DATA FOR THE HYDROGEN BRONZE $HRhO_2$

hkl	d_{obs} (Å)	d_{calc} (Å)	I_{obs}
003	4.455	4.468	100
101	2.629	2.629	36
012	2.481	2.489	80
006	2.253	2.234	9
104	—	2.094	—
015	1.895	1.896	23
107	1.555	1.558	16
110	1.546	1.548	64
009	—	1.489	—
113	1.461	1.462	50
018	—	1.421	—
021	1.337	1.334	30
202	—	1.314	—
116	—	1.272	—
024	—	1.245	—

Note. Intensities *I* given in relative values (%); hexagonal, $a = 3.096$, $c = 13.406$.

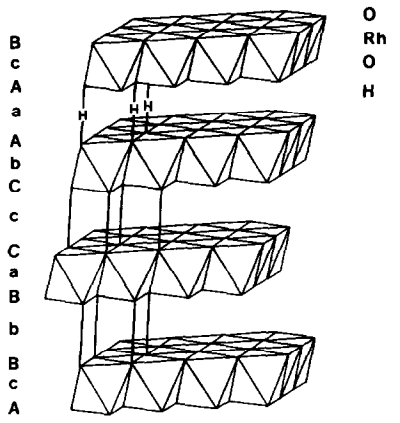

Fig. 6. Structure scheme of $HRhO_2$.

as well as H_2O molecules are available for protonation (Fig. 6).

Conclusions

Kinetic and structural reasons are obviously responsible for the strong differences in reactivity among the alkali oxorhodates $ARhO_2$ investigated. The topotactic exchange and redox properties of phases with oxide layers also are obviously strongly inferior to those of the related alkali transition metal chalcogenides A_xMX_2 (X = S, Se). With respect to solvate exchange and Brönsted acid behavior, the origin of this difference must be attributed (at a similar oxidation state of the transition metal) to the lower acidity of O–H bonds and the higher energy of O–H · · · O hydrogen bonding as compared to the acidity of S–H groups and S–H · · · S (or S–H · · · O) hydrogen bonding. While ternary phases A_xMX_2 can usually be oxidized quantitatively to MS_2, the redox range of ternary layered oxides is limited, and the quantitative oxidation to potential new metastable binary phases MO_2 with layer structure has not yet been observed. This difference is a consequence of the higher ionicity of M–O bonds compared to M–X bonds. In the oxide case, the system relaxes on overoxidation beyond the accessible topotactic range due to increasing electrostatic repulsion M–M by irreversible diffusion of the transition metal ions to lattice sites within the interlayer space, resulting in the formation of either partially ordered new phases or amorphous materials. An example is the quantitative irreversible oxidation of $LiVO_2$ to disordered VO_2, which at 450°C transforms to the rutile-type structure. Similar behavior is found with the oxidation of layered $NaTiO_2$ to the disordered phase $Na_xTi_x\square_{1-x-y}(Ti_{1-y}\square_y)O_2$ (*19–21*).

Acknowledgment

A. Mendiboure and G. V. Subba Rao are indebted to the Alexander von Humboldt-Stiftung for granting a research fellowship.

References

1. A. Lerf and R Schöllhorn, *Inorg. Chem.* **16,** 2950 (1977).
2. G. V. Subba Rao and M. W. Shafer, *in* "Intercalated Materials" (F. Levy Ed.), p. 99, Reidel, Dordrecht/Boston (1979).
3. J. Rouxel, *in* "Intercalated Layered Materials" (F. Levy Ed.), p. 201, Reidel, Dordrecht/Boston (1979).
4. R. Schöllhorn, *in* "Intercalation Chemistry" (M. S. Whittingham and A. J. Jacobson, Eds.), p. 315, Academic Press, New York (1982).
5. M. S. Whittingham, *Prog. Solid State Chem.* **12,** 41 (1978).
6. C. Delmas, J. J. Braconnier, A. Maazaz, and P. Hagenmuller, *Rev. Chem Mineral.* **19,** 343 (1982).
7. A. Mendiboure, C. Delmas, and P. Hagenmuller, *Mater. Res. Bull.* **19,** 1383 (1984).
8. A. Mendiboure, C. Delmas, and P. Hagenmuller, *J. Solid State Chem.* **57,** 323 (1985).
9. M. S. Goldstaub, *C.R. Acad. Sci. Paris* **196,** 280 (1933).
10. V. B. Lazarev and I. S. Shaplygin, *Russ. J. Inorg. Chem.* **23,** 802 (1978).
11. E. F. Bertaut and J. Dulac, *J. Phys. Chem. Solids* **21,** 118 (1961).
12. J. J. Scheer, A. E. van Arkel, and R. D. Heyding, *Canad. J. Chem.* **33,** 683 (1955).

13. R. D. SHANNON AND C. T. PREWITT, *Acta Crystallogr. B* **26,** 1046 (1970).
14. M. GARREAU, J. THEVENIN, AND D. WARIN, *C.R. Acad. Sci. Paris C* **286,** 545 (1978).
15. R. ARNDT AND R. SCHÖLLHORN, *J. Solid State Chem.* **29,** 259 (1979).
16. P. RATHNER, DISSERTATION, UNIV. OF MÜNSTER (FRG) (1986); P. RATHNER AND R. SCHÖLLHORN (IN PREPARATION).
17. R. M. DOUGLASS, *Acta Crystallogr.* **10,** 432 (1957).
18. W. C. HAMILTON AND J. A. IBERS, *Acta Crystallogr.* **16,** 1209 (1963).
19. K. VIDYASAGAR AND J. GOPALAKRISHNAN, *J. Solid State Chem.* **42,** 217 (1982).
20. L. A. DE PICCIOTTO AND M. M. THACKERAY, *Solid State Ionics* **18/19,** 773 (1986).
21. A. MAAZAC, C. DELMAS, AND P. HAGENMULLER, *J. Incl. Phenomena* **1,** 45 (1983).
22. DELIENS AND GOETHALS, *Mineral Mag.* **39,** 152-7 (1973).
23. KONDRASHEV AND FEDOROVA, *Dokl. Akad. Nauk.* **94,** 229 (1954).